

Second harmonic generation in one-dimensional nonlinear photonic crystals solved by the transfer matrix method

Jing-Juan Li, Zhi-Yuan Li,^{*} and Dao-Zhong Zhang

Laboratory of Optical Physics, Institute of Physics, Chinese Academy of Sciences, P. O. Box 603, Beijing 100080, China

(Received 23 October 2006; revised manuscript received 6 February 2007; published 9 May 2007)

The transfer matrix method has been widely used to calculate the scattering of electromagnetic waves. In this paper, we develop the conventional transfer matrix method to analyze the problem of second harmonic generation in a one-dimensional multilayer nonlinear optical structure. In the designed nonlinear photonic crystal structure, the linear and nonlinear optical parameters are both periodically modulated. We have taken into account the multiple reflection and interference effects of both the linear and nonlinear optical waves during the construction of the transfer matrix for each composite layer. Application of this method to multilayer nonlinear photonic crystal structures with different refractive indices indicates that the proposed method is an exact approach and can simulate the generation of the second harmonic field precisely. In an optimum structure, the second harmonic generation efficiency can be several orders of magnitude larger than in a conventional quasi-phase-matched nonlinear structure with the same sample length. The reason is that, due to the presence of photonic band gap edges, the density of states of the electromagnetic fields is large, the group velocity is small, and the local field is enhanced. All three factors contribute to significant enhancement of the nonlinear optical interactions.

DOI: [10.1103/PhysRevE.75.056606](https://doi.org/10.1103/PhysRevE.75.056606)

PACS number(s): 42.70.Qs, 42.65.Ky, 42.79.Nv

I. INTRODUCTION

Since the concept of photonic crystals, materials with a periodic modulation of the refractive index that can give rise to photonic band gaps, was introduced, numerous theoretical approaches have been developed to study photonic crystal structures. These include the plane-wave expansion method [1–3], the transfer matrix method (TMM) [4–7], the finite-difference time-domain method [8,9], and so on. Among them, the TMM, which uses a transfer matrix to connect the electromagnetic (e.m.) fields among different layers, has been widely used to calculate the photonic band structure and transmission and reflection spectra of one-, two-, and three-dimensional photonic crystal structures.

During recent years, periodically poled ferroelectric crystals have attracted much attention because of their unique properties in compensating for the phase mismatch in nonlinear optical interaction processes. Second-order nonlinear optical interactions, such as second harmonic generation (SHG) and the optical parametric oscillator, have been investigated extensively in periodically poled LiNbO₃, LiTaO₃, KTiOPO₄, and strontium barium niobate, respectively [10–14]. However, high-power nonlinear radiation is always a problem difficult to deal with because of limitations such as optical damage. Increase of the nonlinear conversion efficiency is a long-standing goal for periodically poled ferroelectric crystals. Recently, an enhancement by several orders of magnitude of second-order nonlinear interactions in photonic crystals has been reported [15–20]. The enhancement is ascribed to the combination of a high electromagnetic mode density of states and a slowing down of the optical wave at frequencies near the photonic band gap edge, which is induced by multiple reflection and interference. Theoretical

analysis of harmonic generation in layered devices also has gained considerable attention [21–26]. However, up to now, the unique properties of the photonic band gap edge have not been employed in periodically poled materials. Here, we investigate the SH generation in a periodically poled nonlinear crystal with different refractive indices by the transfer matrix method. Because new SH waves generated inside the structure grow as the propagation length increases, the matrix describing the SH wave propagation will be related to the distribution of the pump field of the fundamental waves inside the structure, and must be very complex. So it is difficult to get the matrix describing the SH signal accurately in a multilayered nonlinear optical material.

To reduce the complexity and difficulty of the nonlinear optical problems in an inhomogeneous medium for both the fundamental and SH waves, most existent TMMs that have been adopted to handle nonlinear media have made some kind of approximation and are not thus perfectly accurate. In Ref. [18] the authors used a transfer matrix method to carry out numerical integrations of Maxwell's equations. They assumed a resonant second harmonic field and only a forward-propagating pump wave. They did not consider pump wave reflections because the pump wave was assumed to be tuned away from any resonance and from the band gap edge. This neglect is not valid in the case of deep-grating photonic crystal structures with remarkable modulation of the refractive index of the multilayered composite materials. Reference [22] proposed a transfer matrix method to analyze optical wave interactions through layered nonlinear media. It took into account the internal multiple reflections but neglected the interferences between the forward- and backward-propagating waves. However, it is worth noting that constructive or destructive interferences can greatly change the observed total intensity of fundamental and SH waves, so the approximate approach appears to be problematic, and a more exact theoretical approach is needed.

^{*}Email address: lizy@aphy.iphy.ac.cn

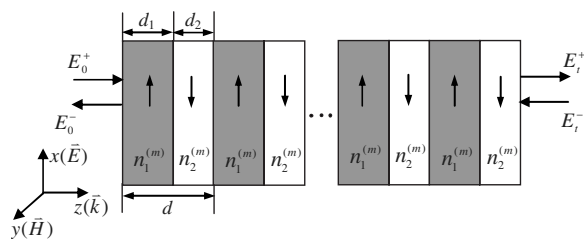


FIG. 1. Schematic diagram of multilayered nonlinear medium. The arrows inside the crystal indicate the direction of spontaneous polarization.

In this paper, we propose a transfer matrix method that can efficiently and accurately deal with a SHG problem where plane-wave fundamental beams are incident upon a multilayered nonlinear medium in which both the linear and nonlinear optical parameters are periodically modulated. The method is free of the aforementioned approximations made in the previous literature. Nevertheless, the current method is also subject to the major limitation that the nonlinear process is assumed to be weak in the sense that the fundamental pump waves are essentially unaffected by the nonlinear processes. Using this approach, we calculate not only the SH energy output but also the distribution of pump and SH fields inside the structure. In our calculation, we make no approximation except for the nondepleted pump wave approximation, and all interferences between all propagating components (including forward- and backward-propagating waves induced by multiple reflections when optical waves propagate through periodic dielectric structures) are included. Our results are different from those for the traditional quasi-phase-matched (QPM) bulk medium and we discuss the reason for this.

II. TMM FOR SHG IN MULTILAYERED STRUCTURES

In this section, we consider a layered periodical nonlinear material with periodically modulated linear and nonlinear optical parameters. The characteristic spatial scales of the variation of the linear refractive index and nonlinear susceptibility are the same. The structure can be divided into N segments of length d , and each segment consists of two homogeneous sections, as depicted in Fig. 1. The length and linear and nonlinear optical parameters for section I are, respectively, d_1 , $n_1^{(m)}$, and $\chi^{(2)}$, while those for section II are d_2 , $n_2^{(m)}$, and $-\chi^{(2)}$, where $m=1, 2$ denotes the fundamental field ($m=1$) and second harmonic field ($m=2$). Because of the mismatch between the refractive indices $n_1^{(m)}$ and $n_2^{(m)}$, there will be reflection at each layer interface, and interference will occur. Now, we begin to study the SHG process in this structure, where e.m. waves of angular frequency ω propagate through the media and new second harmonic waves of frequency 2ω are generated. In our TMM, we simplify the process of SHG into three dependent processes. First, the fundamental field (FF) propagates in the medium and makes the medium polarized; macroscopic polarization is created. Second, the second nonlinear polarization P^{NL} induced by the nonlinear medium radiates a second harmonic (SH) field.

Third, the SH field created inside the medium propagates in the structure and radiates from the medium as SH signals.

Now, we analyze the propagation of the FF. We suppose a plane e.m. wave with frequency ω is incident from the left-hand side of the structure. Let the wave propagate along the z -axis direction and the polarization of the electric field be along the x axis. The fundamental-wave electric field in each homogeneous medium can be written as

$$E_i^{(1)}(z, t) = \Omega_i^+ \exp\{i[k_i^{(1)}(z - z_{i-1}) - \omega t]\} + \Omega_i^- \exp\{-i[k_i^{(1)}(z - z_{i-1}) - \omega t]\}, \quad (1)$$

where z_0 is set as 0, $z_i = z_{i-1} + d_i$, $k_i^{(1)} = n_i^{(1)}k_{10}$, and $k_{10} = \omega/c$. c is the light speed in vacuum. Ω_i^\pm is the complex electric-field amplitude at the interface and the sign $+(-)$ denotes the forward- (backward-)propagating wave. Using the continuity condition of the E and H fields at the layer boundary, we can get the following relationship between the amplitudes of the E field across the odd-even interface:

$$\begin{pmatrix} \Omega_{2i-1}^+ \\ \Omega_{2i-1}^- \end{pmatrix} = \frac{1}{2n_1^{(1)}} \begin{pmatrix} n_1^{(1)} + n_2^{(1)} & n_1^{(1)} - n_2^{(1)} \\ n_1^{(1)} - n_2^{(1)} & n_1^{(1)} + n_2^{(1)} \end{pmatrix} \begin{pmatrix} \Omega_{2i}^+ \\ \Omega_{2i}^- \end{pmatrix} = T_{12} \begin{pmatrix} \Omega_{2i}^+ \\ \Omega_{2i}^- \end{pmatrix}. \quad (2)$$

Defining $D_1 = \begin{pmatrix} 1 & 1 \\ n_1^{(1)} & -n_1^{(1)} \end{pmatrix}$ and $D_2 = \begin{pmatrix} 1 & 1 \\ n_2^{(1)} & -n_2^{(1)} \end{pmatrix}$ we can write T_{12} as

$$T_{12} = D_1^{-1} D_2.$$

Similarly, we can get the relationship between the amplitudes of the E field across the even-odd interface:

$$T_{21} = D_2^{-1} D_1.$$

The phase and amplitude changes in the fields from the left-hand side to the right-hand side of a homogeneous layer can be described as

$$P_j = \begin{pmatrix} \exp(ik_j^{(1)}d_j) & 0 \\ 0 & \exp(-ik_j^{(1)}d_j) \end{pmatrix},$$

$j = 1, 2$ denoting the odd and even layer, respectively.

The overall transfer matrix of the multilayer structure is obtained from the cascading product of the successive individual transfer matrices of each layer:

$$T = D_0^{-1} (D_2 P_2 D_2^{-1} D_1 P_1 D_1^{-1})^N D_0, \quad (3)$$

where $D_0 = \begin{pmatrix} 1 & 1 \\ n_0 & -n_0 \end{pmatrix}$, and n_0 is the refractive index of the air background. The FFs in the right and left sides of the structure are related by this matrix:

$$\begin{pmatrix} \Omega_t^+ \\ \Omega_t^- \end{pmatrix} = T \begin{pmatrix} \Omega_0^+ \\ \Omega_0^- \end{pmatrix}. \quad (4)$$

From this equation one can solve for the reflection and transmission coefficients (Ω_0^- and Ω_t^+) under a given incident wave coefficient (Ω_0^+). Then, the relative amplitudes Ω_t^\pm of every layer can be completely determined from the incident, reflection, and transmission coefficients:

$$\begin{pmatrix} \Omega_{2i-1}^+ \\ \Omega_{2i-1}^- \end{pmatrix} = D_{2i-1}^{-1} (D_2 P_2 D_2^{-1} D_1 P_1 D_1^{-1})^{i-1} D_0 \begin{pmatrix} \Omega_0^+ \\ \Omega_0^- \end{pmatrix}, \quad (5)$$

$$\begin{pmatrix} \Omega_{2i}^+ \\ \Omega_{2i}^- \end{pmatrix} = D_{2i}^{-1} D_1 P_1 D_1^{-1} (D_2 P_2 D_2^{-1} D_1 P_1 D_1^{-1})^{i-1} D_0 \begin{pmatrix} \Omega_0^+ \\ \Omega_0^- \end{pmatrix}. \quad (6)$$

Now that we have obtained the distribution of the FF everywhere within the nonlinear optical medium, we have accomplished the first process in our TMM. Let us move on to the second process, where the solution of the SH field within every composite layer is the central task. The nonlinear polarization induced by the FF inside each layer is directly related to the fundamental field as

$$P_i^{NL}(z, t) = \varepsilon_0 \chi_i^{(2)} [E_i^{(1)}(z)]^2 \exp(-i2\omega t). \quad (7)$$

In the solution to the propagation equation of the SH field, we retain all second-order spatial derivatives, and our result is free from the usual slowly-varying-amplitude approximation. The propagation equation for the SH field is

$$\frac{\partial^2 E_{2\omega}(z)}{\partial z^2} + k_2^2 E_{2\omega}(z) = \mu \frac{\partial^2 P^{NL}(z, t)}{\partial t^2}. \quad (8)$$

In each layer of the composite structure Eq. (8) becomes

$$\begin{aligned} \frac{\partial^2 E_i^{(2)}(z)}{\partial z^2} + k_i^{(2)2} E_i^{(2)}(z) \\ = -\mu \varepsilon_0 \chi_i^{(2)} 4\omega^2 \{(\Omega_i^+)^2 \exp[2ik_i^{(1)}(z - z_i)] + 2\Omega_i^+ \Omega_i^- \\ + (\Omega_i^-)^2 \exp[-2ik_i^{(1)}(z - z_i)]\}, \end{aligned} \quad (9)$$

where $k_i^{(2)}$ and $k_i^{(1)}$ are the wave vectors of the SH field and FF in the i th layer, respectively, and $k_i^{(2)} = n_i^{(2)} k_{20}$, $k_{20} = 2\omega/c$.

By solving Eq. (9), we can get the electric field distribution of the SH wave. In the i th layer, it can be expressed as

$$\begin{aligned} E_i^{(2)}(z) = E_i^{(2)+} \exp[ik_i^{(2)}(z - z_{i-1})] + E_i^{(2)-} \exp[-ik_i^{(2)}(z - z_{i-1})] \\ + A_i (\Omega_i^+)^2 \exp[i2k_i^{(1)}(z - z_{i-1})] \\ + A_i (\Omega_i^-)^2 \exp[-i2k_i^{(1)}(z - z_{i-1})] + 2C_i \Omega_i^+ \Omega_i^-, \end{aligned} \quad (10)$$

where $E_i^{(2)+}$ and $E_i^{(2)-}$ represent the amplitudes of the forward and backward SH waves, and $A_i = \frac{-4\mu\varepsilon_0\chi_i^{(2)}\omega^2}{k_i^{(2)2} - 4k_i^{(1)2}}$, $C_i = \frac{-4\mu\varepsilon_0\chi_i^{(2)}\omega^2}{k_i^{(2)2}}$.

Using the Maxwell equations, we can write the magnetic field H in the i th layer as

$$\begin{aligned} H_i^{(2)}(z) = \frac{1}{ik_{20}} [\nabla \times E_i^{(2)}(z)] \\ = n_i^{(2)} \{E_i^{(2)+} \exp[ik_i^{(2)}(z - z_{i-1})] \\ - E_i^{(2)-} \exp[-ik_i^{(2)}(z - z_{i-1})]\} \\ + \frac{2k_{10}n_i^{(1)}}{k_{20}} A_i \{(\Omega_i^+)^2 \exp[i2k_i^{(1)}(z - z_{i-1})] \\ - (\Omega_i^-)^2 \exp[-i2k_i^{(1)}(z - z_{i-1})]\}, \end{aligned} \quad (11)$$

where $k_{10} = \omega/c$ and $k_{20} = 2\omega/c$ are the wave vectors of the FF and SH waves in the air, respectively.

After we get the electric [Eq. (10)] and magnetic [Eq. (11)] fields of the SH within every layer, it is time to deal with the last process, namely, to study the propagation of the SH. For the sake of convenience we make the following definitions:

$$E_i^{(2)+}(z) = E_i^{(2)+} \exp[ik_i^{(2)}(z - z_{i-1})],$$

$$E_i^{(2)-}(z) = E_i^{(2)-} \exp[-ik_i^{(2)}(z - z_{i-1})],$$

$$(\Omega_i^+)^2(z) = (\Omega_i^+)^2 \exp[i2k_i^{(1)}(z - z_{i-1})],$$

$$(\Omega_i^-)^2(z) = (\Omega_i^-)^2 \exp[-i2k_i^{(1)}(z - z_{i-1})].$$

Then Eqs. (10) and (11) can be written in the form of a matrix as

$$\begin{aligned} \begin{pmatrix} E_i^{(2)+}(z) \\ H_i^{(2)}(z) \end{pmatrix} = \begin{pmatrix} 1 & 1 \\ n_i^{(2)} & -n_i^{(2)} \end{pmatrix} \begin{pmatrix} E_i^{(2)+}(z) \\ E_i^{(2)-}(z) \end{pmatrix} \\ + \begin{pmatrix} 1 & 1 \\ \frac{2n_i^{(1)}k_{10}}{k_{20}} & -\frac{2n_i^{(1)}k_{10}}{k_{20}} \end{pmatrix} \begin{pmatrix} A_i (\Omega_i^+)^2(z) \\ A_i (\Omega_i^-)^2(z) \end{pmatrix} \\ + \begin{pmatrix} 1 \\ 0 \end{pmatrix} C_i \Omega_i^+ \Omega_i^-. \end{aligned} \quad (12)$$

In Eq. (12), the first part on the right side of the equation denotes the free-wave amplitudes of the SH e.m. fields, the second part denotes the bound-wave amplitudes of the SH fields just created by the forward and backward FFs in this layer, and the third part denotes the influence of interference between the forward and backward FFs on the SH fields.

For convenience, we define several matrices as

$$G_0 = \begin{pmatrix} 1 & 1 \\ n_{20} & -n_{20} \end{pmatrix}, \quad G_1 = \begin{pmatrix} 1 & 1 \\ n_1^{(2)} & -n_1^{(2)} \end{pmatrix},$$

$$G_2 = \begin{pmatrix} 1 & 1 \\ n_2^{(2)} & -n_2^{(2)} \end{pmatrix}, \quad B_1 = \begin{pmatrix} 1 & 1 \\ \frac{2n_1^{(1)}k_{10}}{k_{20}} & -\frac{2n_1^{(1)}k_{10}}{k_{20}} \end{pmatrix},$$

$$B_2 = \begin{pmatrix} 1 & 1 \\ \frac{2n_2^{(1)}k_{10}}{k_{20}} & -\frac{2n_2^{(1)}k_{10}}{k_{20}} \end{pmatrix}.$$

We will now determine the values of the free-wave amplitudes $E_i^{(2)+}$ and $E_i^{(2)-}$. Considering the continuous condition of the electric and magnetic fields at the interfaces $Z = Z_{2(j-1)}$, $Z = Z_{2j-1}$, and $Z = Z_{2j}$, we get the relation of the SH field through the j th segment ($j = 1, 2, \dots, N$):

$$\begin{aligned}
\begin{pmatrix} E_j^{(2)+} \\ E_j^{(2)-} \end{pmatrix} &= G_0^{-1} S G_0 \begin{pmatrix} E_{j-1}^{(2)+} \\ E_{j-1}^{(2)-} \end{pmatrix} + G_0^{-1} (N_2 B_1 F_1 - S B_1) \\
&\times \begin{pmatrix} A_1 (\Omega_{2j-1}^+)^2 \\ A_1 (\Omega_{2j-1}^-)^2 \end{pmatrix} + G_0^{-1} (N_2 - S) \begin{pmatrix} 1 \\ 0 \end{pmatrix} C_1 \Omega_{2j-1}^+ \Omega_{2j-1}^- \\
&+ G_0^{-1} (B_2 F_2 - N_2 B_2) \begin{pmatrix} A_2 (\Omega_{2j}^+)^2 \\ A_2 (\Omega_{2j}^-)^2 \end{pmatrix} + G_0^{-1} (1 - N_2) \\
&\times \begin{pmatrix} 1 \\ 0 \end{pmatrix} C_2 \Omega_{2j}^+ \Omega_{2j}^-, \quad (13)
\end{aligned}$$

where $S = G_2 Q_2 G_2^{-1} G_1 Q_1 G_1^{-1}$, $N_2 = G_2 Q_2 G_2^{-1}$,

$$Q_1 = \begin{pmatrix} \exp(ik_1^{(2)} d_1) & 0 \\ 0 & \exp(-ik_1^{(2)} d_1) \end{pmatrix},$$

$$Q_2 = \begin{pmatrix} \exp(ik_2^{(2)} d_2) & 0 \\ 0 & \exp(-ik_2^{(2)} d_2) \end{pmatrix},$$

$$F_1 = \begin{pmatrix} \exp(i2k_1^{(1)} d_1) & 0 \\ 0 & \exp(-i2k_1^{(1)} d_1) \end{pmatrix},$$

$$F_2 = \begin{pmatrix} \exp(i2k_2^{(1)} d_2) & 0 \\ 0 & \exp(-i2k_2^{(1)} d_2) \end{pmatrix}.$$

As a recursive equation, Eq. (13) serves as the unit transfer matrix of the SH field for the j th segment. From this equation we can get the overall transfer matrix of the SH signal for the whole nonlinear structure. Considering the periodicity of the structure, we get the SH fields radiated from the left and right sides of the multilayered nonlinear structure composed of N segments by recursion:

$$\begin{aligned}
\begin{pmatrix} E_t^{(2)+} \\ 0 \end{pmatrix} &= G_0^{-1} S^N G_0 \begin{pmatrix} 0 \\ E_0^{(2)-} \end{pmatrix} \\
&+ \sum_{i=1}^N G_0^{-1} S^{N-i} \left[(N_2 B_1 F_1 - S B_1) \begin{pmatrix} A_1 (\Omega_{2i-1}^+)^2 \\ A_1 (\Omega_{2i-1}^-)^2 \end{pmatrix} \right. \\
&+ (N_2 - S) \begin{pmatrix} 1 \\ 0 \end{pmatrix} C_1 \Omega_{2i-1}^+ \Omega_{2i-1}^- + (B_2 F_2 - N_2 B_2) \\
&\left. \times \begin{pmatrix} A_2 (\Omega_{2i}^+)^2 \\ A_2 (\Omega_{2i}^-)^2 \end{pmatrix} + (1 - N_2) \begin{pmatrix} 1 \\ 0 \end{pmatrix} C_2 \Omega_{2i}^+ \Omega_{2i}^- \right]. \quad (14)
\end{aligned}$$

From Eq. (14) we can calculate $E_0^{(2)-}$ (the SH field radiated from the left side) and $E_t^{(2)+}$ (the SH field radiated from the right side). Using the same method we can also get the SH field distribution inside the structure.

III. RESULTS AND DISCUSSION

In the following calculation, we assume that the multilayered media are composed of periodically poled strontium barium niobate (SBN) crystal, whose nonlinear susceptibility is $\chi^{(2)} = 27.2$ pm/V. The refractive index for SBN is given by the following dispersion formula:

$$n^2 = a + \frac{b}{\lambda^2 - c} + d\lambda,$$

where $a = 4.78 + 0.38x$, $b = 1.02 \times 10^5 + 1.48 \times 10^4 x$, $c = 4.72 \times 10^4 + 2.67 \times 10^4 x$, $d = -2.14 \times 10^{-5} x$, and $x = 0.75$. The wavelength λ is in units of nanometers.

Periodically poled ferroelectric crystals are characterized by modulations of the nonlinear susceptibilities. In order to introduce photonic band gaps, we use the electro-optical effect of this crystal to realize the modulation of the refractive index. If an electric field E is applied along the optical axis the new refractive index is

$$n_1 = n + \Delta n_1 = n - \frac{1}{2} n^3 r_{33} E,$$

where r_{33} is the electro-optic coefficient of the material and E is the electric field amplitude. Similar to the nonlinear optical coefficient, the electro-optic coefficient also has different signs in different domains. Therefore, in the reversed domains, the electro-optic coefficient changes sign and the refractive index can be written as

$$n_2 = n + \Delta n_2 = n + \frac{1}{2} n^3 r_{33} E.$$

It is obvious that a modulated linear susceptibility occurs due to the presence of an external strong electric field based on the electro-optical effect. As a result, photonic band gaps may become available in periodically poled ferroelectric crystals.

If there is only a modulation of nonlinear susceptibility while the linear refractive indices are uniform, the conversion efficiency will be modulated by the phase difference between the FF and SH field. The maximal conversion efficiency will be achieved when the quasi-phase-matched condition is satisfied. But when there are large refractive index discontinuities, the phase of the transmitted plane-wave field will undergo a shift at the boundary. The wave vectors are also strongly modified because of the appearance of photonic band gaps. As a result, the original QPM condition is violated and the conventional QPM mechanism must be rewritten in the new nonlinear photonic crystal structures. Although a Bloch wave can be defined in this structure, which has a periodic refractive index modulation [27], and with the nondepleted pump wave approximation the FF can be represented by the Bloch wave, yet for the generated SH wave, a Bloch wave representation is inappropriate for several reasons. First, the forward Bloch wave is subject to reflection at the sample surface. More importantly, the SH wave radiated from the nonlinear polarization created by the Bloch wave will encounter significant multiple reflection within the remarkably modulated photonic crystal structure. Finally, the SH wave is also subject to reflection at the sample surface. It is then clear that a Bloch wave is not the most appropriate tool to accurately describe the nonlinear optical interactions in the current structure. It is very difficult to extract an explicit expression for the phase match condition from such a picture.

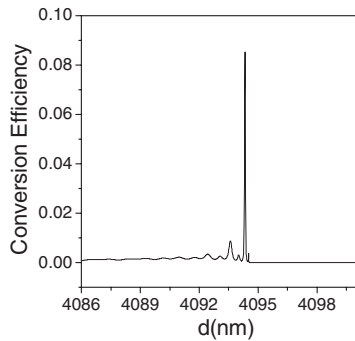


FIG. 2. Conversion efficiency of second harmonic wave vs thickness of each segment, d . the maximum conversion efficiency occurs when $d=4094.33$ nm and $d_1=3363.162$ nm. The wavelength of the pump wave is $\lambda=848.0$ nm.

It can be seen clearly from the rather messy mathematical derivation in Sec. II that the existence of a strong light scattering effect in the nonlinear photonic crystal structure has greatly complicated the analysis of the SHG problem. It is obvious that the conventional analytical solution used in the usual QPM problem is no longer valid. Because of this, we directly carry out numerical simulations to establish the QPM condition of the structure by tuning the thickness of the two composite domains. The optimum structure is judged by occurrence of the maximum SH conversion efficiency. In Fig. 2 we plot the SH conversion efficiency as a function of the thickness of each segment d , when the thickness of the positive domain is set to $d_1=3363.162$ nm. The structure is composed of 50 layer-pair stacks, and we choose the fundamental light wavelength as 848.0 nm. For this wavelength, the refractive indices in the positive and negative domains are $n_1^{(1)}=1.617$ and $n_2^{(1)}=2.955$, respectively, after applying an external electric field whose intensity is of the order of tens of kV/mm. The refractive indices of the SH wave in the positive and negative domains are $n_1^{(2)}=1.68$ and $n_2^{(2)}=3.245$, respectively. A smaller electric field will lead to shallower modulation of the refractive index. However, the design principle is the same. We note from Fig. 2 that the maximum SH conversion efficiency occurs when $d=4094.33$ nm and the maximum value of conversion efficiency is about 10%. This is quite remarkable considering the fact that the total length of the structure is only about $205 \mu\text{m}$. In the structure described above, a minimization of the phase difference between the FF and SH waves must be reached. Otherwise, if the phase is totally mismatched, the SH field cannot constructively grow in the whole length of the structure and the efficiencies are often of the order of magnitude of 10^{-5} .

It is well known that the SH conversion efficiency is determined not only by the power of the pump light, but also by the intensity of the pump light inside the media. So, except for the QPM condition, the properties of photonic band edges contribute much to the enhancement of SH conversion efficiency. Figure 3(a) plots the SH conversion efficiency as a function of pump field intensity. The conversion efficiency is defined as the ratio between the light intensities of the SH and fundamental pump waves. As a comparison, the SH conversion efficiency from a QPM SBN crystal of equivalent

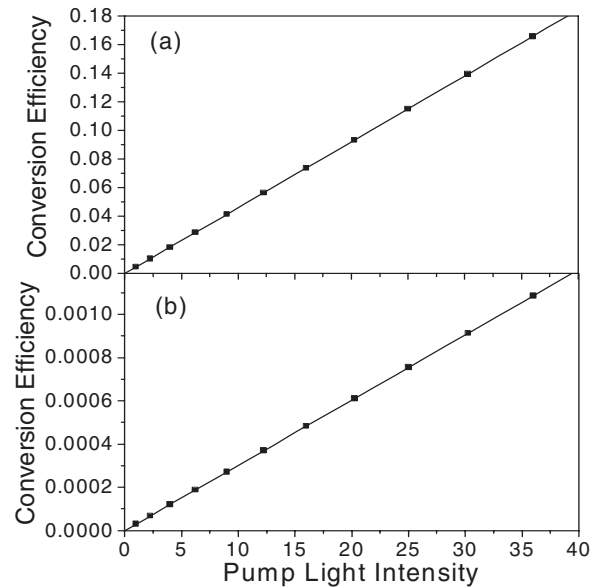


FIG. 3. Second harmonic wave conversion efficiency vs pump light intensity: (a) the optimized layered structure with periodic poling; (b) QPM uniform bulk crystal. The squares represent calculated values and the solid line is a linear fit. The structure of (a) is the same as that of Fig. 2.

length is shown in Fig. 3(b). The conversion efficiency in Fig. 3(b) is just on the order of 10^{-3} , which is lower by two orders of magnitude than the value of the designed structure as discussed in Fig. 2. Figure 4 illustrates the calculated transmittance spectrum for $d=4094.33$ nm. Material disper-

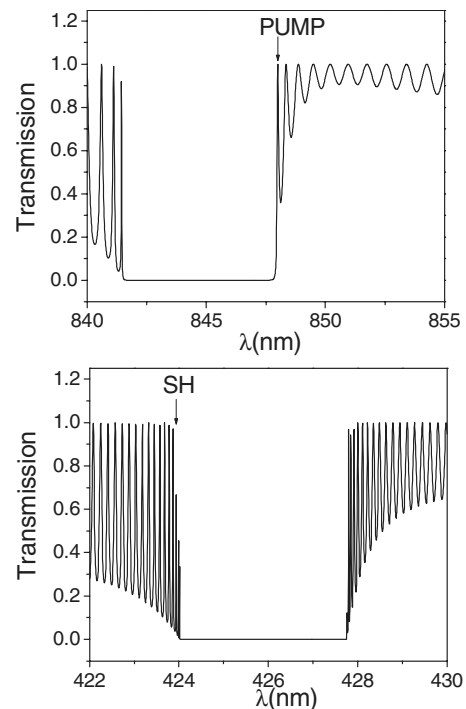


FIG. 4. Transmission spectra around the fundamental and second harmonic field wavelengths when $d=4094.33$ nm, which is the optimized structure to generate the second harmonic waves obtained through Fig. 2.

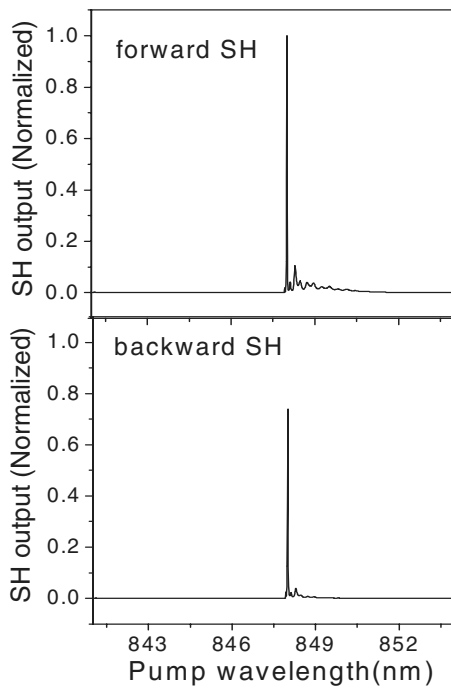


FIG. 5. SH output (normalized) vs wavelength of pump waves. The parameters of the nonlinear optical structure are the same as those in Fig. 4.

sion has been considered in the numerical calculation. The result suggests that this choice of parameters has resulted in a situation where the FF and SH signals are all located at the photonic band gap edges, where the density of electromagnetic field modes is large and the group velocity is low. Therefore, the field amplitude may be enhanced by one order of magnitude or more, and the nonlinear interaction time becomes much longer. The combination of these several factors is ultimately responsible for the greatly enhanced efficiencies.

Figure 5 plots the calculation results of the SHG efficiency when detuning the pump wave around 848.0 nm. The nonlinear optical structure is identical to that in Fig. 4. The left and right curves denote the forward and backward output intensity, respectively. Each vertical axis scale is defined on each side of the figure. The amplitude in the figure has been normalized to unity. It can be seen from Fig. 5 that the structure proposed here radiates significantly in both directions. The intensity of the backward SH signal is large and approximately equal to that of the forward SH signal, while in the case of an equivalent length of a bulk QPM nonlinear optical medium, the backward signal is lower by one or more orders of magnitude than the forward signal. It is so weak that it is often neglected. The multiple reflection effects induced by large index discontinuity generate the large backward signals as well as the enhanced SH conversion efficiency. The maximum SH signal in this figure corresponds to the band gap edge in Fig. 4, and the ripples near the radiation peak are induced by the multiple reflection effect at the two surfaces of the nonlinear structure.

In order to look straightforwardly at the distribution of fields inside the structure, we plot in Fig. 6 the intensity of the pump field and SH field inside the structure calculated by

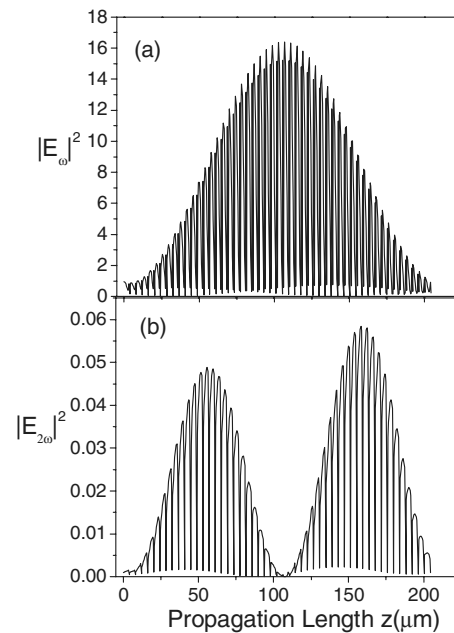


FIG. 6. Light intensity distribution of pump wave and SH wave inside the structure at pump wavelength of 848.0 nm. The maximum field intensity of the pump wave is amplified more than ten times compared to the incident wave.

the proposed TMM. From the figure we can see that the intensity of the pump field is oscillating inside the structure because of the interference induced by multiple reflections. The maximum intensity is enhanced by more than one order of magnitude compared to the incident field amplitude. The enhancement magnitude at different wavelengths is different and is consistent with the transmission spectrum of the pump field as illustrated in Fig. 7, which records the maximum value of the pump intensity inside the structure. The enhancement factor at $\lambda=848.0$ nm is maximal because this wavelength is located at the band gap edge as can be found in Fig. 4. Each wavelength corresponding to the transmission resonance peak in Fig. 4 will have a peak in Fig. 7. However,

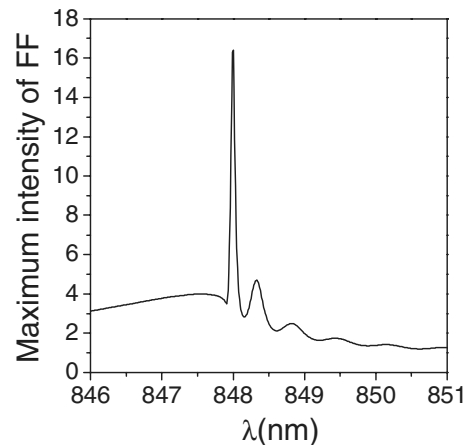


FIG. 7. Maximum value of the pump field intensity inside the structure vs wavelength of pump field. The values of the parameters of the structure are the same as those in Fig. 4.

the farther away the pump wavelength from the band edge, the smaller the peak value of the SH efficiency.

IV. CONCLUSIONS

In summary, we have developed a transfer matrix method to analyze the SHG problem in multilayered nonlinear optical media. Multiple reflection and interference effects are taken into account while deriving the transfer matrix for both the fundamental and SH waves. The proposed method is free from the several major approximations made in the previous literature that handled the harmonic generation problem in conventional QPM nonlinear optical media. To this extent, it is an exact approach and can give accurate results. Using the method, we have investigated the radiation of SH waves from both sides of a nonlinear optical sample and the distribution of SH fields within the structure. As an example, we have investigated SHG in a one-dimensional SBN nonlinear photonic crystal. Comparison has been made between the current designed and the conventional QPM structure. It is

found that, in an optimum structure, the second harmonic generation efficiency can be several orders of magnitude larger than in a conventional QPM nonlinear structure with the same sample length. The reason is that, due to the presence of photonic band gap edges, the density of states of the electromagnetic fields is large, the group velocity is small, and the local field is enhanced. All three factors contribute to the significant enhancement of nonlinear optical interactions. In addition to the usual SHG from the forward direction of the pump wave, the SHG from the backward direction is also strong due to the large scattering effect by the nonlinear photonic crystal.

ACKNOWLEDGMENTS

The authors would like to acknowledge the financial support of the National Natural Science Foundation of China through Grants No. 10404036 and No. 10474135, and the National Key Basic Research Special Foundation of China through Grant No. 2006CB921702.

-
- [1] K. M. Ho, C. T. Chan, and C. M. Soukoulis, *Phys. Rev. Lett.* **65**, 3152 (1990).
- [2] D. Cassagne, C. Jouanin, and D. Bertho, *Phys. Rev. B* **53**, 7134 (1996).
- [3] Z. Y. Li, J. Wang, and B. Y. Gu, *Phys. Rev. B* **58**, 3721 (1998).
- [4] J. B. Pendry, *J. Mod. Opt.* **41**, 209 (1994).
- [5] P. M. Bell, J. B. Pendry, L. Marin Moreno, and A. J. Ward, *Comput. Phys. Commun.* **85**, 306 (1995).
- [6] Z. Y. Li and L. L. Lin, *Phys. Rev. E* **67**, 046607 (2003).
- [7] L. L. Lin, Z. Y. Li, and K. M. Ho, *J. Appl. Phys.* **94**, 811 (2003).
- [8] C. T. Chan, Q. L. Yu, and K. M. Ho, *Phys. Rev. B* **51**, 16635 (1995).
- [9] A. Taflove and S. C. Hagness, *Computational Electrodynamics: The Finite-Difference Time-Domain Method* (Artech House, Norwood, MA, 2000).
- [10] P. Xu, S. H. Ji, S. N. Zhu, X. Q. Yu, J. Sun, H. T. Wang, J. L. He, Y. Y. Zhu, and N. B. Ming, *Phys. Rev. Lett.* **93**, 133904 (2004).
- [11] P. Ni, B. Ma, X. Wang, B. Cheng, and D. Zhang, *Appl. Phys. Lett.* **82**, 4230 (2003).
- [12] L. E. Myers, R. C. Eckardt, M. M. Fejer, and R. L. Byer, *J. Opt. Soc. Am. B* **12**, 2102 (1995).
- [13] A. Piskarskas, V. Smilgevičius, A. Stabinis, V. Jarutis, V. Pasiskevicius, S. Wang, J. Tellefsen, and F. Laurell, *Opt. Lett.* **24**, 1053 (1999).
- [14] Y. Y. Zhu, J. S. Fu, R. F. Xiao, and G. K. Wong, *Appl. Phys. Lett.* **70**, 1793 (1997).
- [15] Y. Dumeige, P. Vidakovic, S. Sauvage, I. Sagnes, J. A. Levenson, C. Sibia, M. Centini, G. D'Aguanno, and M. Scalora, *Appl. Phys. Lett.* **78**, 3021 (2001).
- [16] A. V. Balakin, V. A. Bushuev, N. I. Koroteev, B. I. Mantsyzov, I. A. Ozheredov, and A. P. Shkurinov, *Opt. Lett.* **24**, 793 (1999).
- [17] J. Torres, D. Coquillat, R. Legros, J. P. Lascaray, F. Teppe, D. Scalbert, D. Peyrade, Y. Chen, O. Briot *et al.*, *Phys. Rev. B* **69**, 085105 (2004).
- [18] J. Martorell and R. Corbalan, *Opt. Commun.* **108**, 319 (1994).
- [19] G. T. Kiehne, A. E. Kryukov, and J. B. Ketterson, *Appl. Phys. Lett.* **75**, 1676 (1999).
- [20] G. Vecchi, J. Terres, D. Coquillat, and M. L. V. d'Yerville, *Appl. Phys. Lett.* **84**, 1245 (2004).
- [21] N. Hashizume, M. Ohashi, T. Kondao, and R. Ito, *J. Opt. Soc. Am. B* **12**, 1894 (1995).
- [22] Yoonchan Jeong and Byoung-ho Lee, *IEEE J. Quantum Electron.* **35**, 162 (1999).
- [23] J. M. Bendickson, J. P. Dowling, and M. Scalora, *Phys. Rev. E* **53**, 4107 (1996).
- [24] M. F. Steel and C. Martijn de Sterke, *Appl. Opt.* **35**, 3211 (1996).
- [25] D. S. Bethune, *J. Opt. Soc. Am. B* **6**, 910 (1989).
- [26] D. S. Bethune, *J. Opt. Soc. Am. B* **8**, 367 (1991).
- [27] A. Yariv and P. Yeh, *Optical Waves in Crystals* (Wiley, New York, 1984).